

# RF MEMS-Based Biosensor for Pathogenic Bacteria Detection

Chithra · Pallavi S. · A. Amalin Prince

Published online: 20 June 2013  
© Springer Science+Business Media New York 2013

**Abstract** A biosensor which is used for determining the concentration of substances and other parameters of biological interest is an integral part of the public health systems. Micromachined sensors based on radio frequency–microelectromechanical systems are an emerging field of study for biosensing applications. In this work, we propose a novel detection method for pathogenic bacteria using a coplanar waveguide (CPW) as well as distributed microelectromechanical systems transmission line (DMTL). *Escherichia coli* has been chosen for the study due to the widespread food poisoning outbreaks caused by its infective strains. But, the model can be easily extended to other pathogenic bacteria as well. The *E. coli* bacterium was modeled as a three-shell structure based on the electrical properties of the *E. coli* cell. An initial study was done using a CPW. The scattering parameters and voltage standing wave ratio were analyzed and found to vary as the number of bacteria positioned on the CPW increased. Reflection parameters were found to have more deviation than the transmission parameters. DMTL was designed by introducing periodic structures in CPW, to allow increased interaction between the electromagnetic waves and the measurand. This improved the quality factor of the resonant peaks in reflection coefficient, thereby allowing us to correlate the number of bacteria to the shift in resonant frequency. Selectivity towards *E. coli* bacteria can be achieved by immobilizing a functionalization layer of anti *E. coli* antibody on the central conductor of

CPW/DMTL. With sufficient calibration, this method can be used to detect and measure the concentration of other pathogenic bacteria as well.

**Keywords** Microelectromechanical systems · RF MEMS · Biosensor · Bacteria detection

## 1 Introduction

The term “biosensor” indicates sensor devices used for determining the concentration of substances and other parameters of biological interest. A biosensor which can detect and quantitatively analyze biological samples with high reliability is very crucial for the biomedical field. The field of biosensors is witnessing immense researches and innovations, for a low-cost portable sensor with higher selectivity and lower response time, which can be easily operated by an individual of average familiarity with the medical field. Conventional optical and chemical methods of biological specimen detection have various drawbacks such as altering of the specimen, attachment of labels, and more response time [1]. However, in situations of a critical disease outbreak, any time delay in identifying the bacteria can prove to be risky and has its far-reaching effects on public health systems as well as industrial food processing centers.

The application of micromachined sensors for chemical/biological specimen detection is a growing area of research [2–4]. These sensors have lower power consumption, faster response, smaller size, easy portability, more efficiency, and capability of working in harsh environments [5]. Based on their sensing mechanism, micromachined biosensors are divided into electrochemical, microcantilever, and dielectric sensors. Though work on both microcantilever and electrochemical biosensors is available in literature, limited work has been done so far on radio frequency–microelectromechanical system (RF MEMS)-based dielectric sensor for pathogenic

---

Chithra (✉) · P. S. · A. A. Prince  
Electrical, Electronics and Instrumentation Engineering  
Department, BITS Pilani, K. K. Birla Goa Campus,  
Zuarinagar, Goa 403726, India  
e-mail: chithrajayarajmm@gmail.com

P. S.  
e-mail: pallu2021@gmail.com

A. A. Prince  
e-mail: amalinprince@gmail.com

bacteria detection. One of the merits of the RF MEMS-based dielectric sensor is the compatibility for integration with microfluidic systems due to single-sided planar configuration.

Here, we propose an RF MEMS-based dielectric sensor for detection of *Escherichia coli* bacteria. As seen in Fig. 1 (courtesy of CDC/National Escherichia, Shigella, Vibrio Reference Unit at CDC), *E. coli* is a rod-shaped bacterium, commonly found in the gut of warm-blooded animals.

It constitutes about 0.1 % of the gut flora. Around 700 strains of *E. coli* have been identified so far. They are classified on the basis of the “O” and “H” antigens found on their cell surface. Though most *E. coli* strains are harmless, some serotypes can cause severe food poisoning. Strains of *E. coli*, such as O157:H7, produce potentially lethal toxins. Food poisoning caused by *E. coli* can result from eating unwashed vegetables, undercooked meat, contaminated water, and unpasteurized milk. *E. coli* can cause gastrointestinal distress, diarrhea, neonatal meningitis, and hemolytic uremic syndrome which can be a severe medical emergency if not treated. Majority of the people who are infected recover within 5 to 7 days without any medical treatment. However, young children, the elderly, and those with weakened immune system are more vulnerable and may have to be hospitalized if symptoms are severe.

Outbreaks have occurred in many developed countries, including Canada, Europe, Australia, and Japan [6, 7]. *E. coli* bacteria have also resulted in massive product recalls in the past. Some of them are Nestlé's Toll House cookie dough recalls (2009) [8], recall of ground beef products by the National Beef Packing Company in the USA (2011) [9], and recall of ready packed salad products by “Ready Pac Foods,” USA (2011).

The fecal–oral transmission is the major route through which a pathogenic strain of the bacterium causes disease. Cells are able to survive outside the body for a limited amount of time. Hence, presence of *E. coli* strain is considered as an indication of fecal contamination. Due to the above reasons, sensing and identification of the *E. coli* bacteria are of immense importance. The food poisoning

outbreaks and product recalls due to *E. coli* also underline this fact.

The standard detection process of *E. coli* bacteria in food processing takes about 24 h [1]. A sample is taken to the lab and placed on a nutrient agar. If *E. coli* are present, they will multiply on the agar, and researchers can visibly identify them. MEMS-based amperometric detection of *E. coli* was achieved by Jen-Jr Gau et al. [10] using self-assembled monolayers of the protein streptavidin immobilized on an electrode array to capture the rRNA from *E. coli*. Another proposed approach is to coat a microcantilever with antibodies that bind the *E. coli* bacteria. When bacteria bind to the microcantilever, its effective mass changes resulting in changes in the resonant frequency of the cantilever vibration [11, 12]. A biosensor based on a fluorescent sandwich immunoassay performed inside a glass capillary optical waveguide has been demonstrated by Peixuan Zhu et al. [13]. Langsite SH SAW sensor by Eric et al. [14], functionalized Si microchannel immunosensor by Roy et al. [15], tin oxide nanowire coupled with microfluidic chip by XingJiu et al. [16], impedance biosensor by Dastider et al. [17], and carbon nanotube-based electrochemical sensor by Jun-Yong et al. [18] are among the different methods proposed for *E. coli* detection [19, 20]. These sensing methods are an improvement over the conventional methods of *E. coli* sensing. However, in microcantilever sensors, even a small change in amplitude of the exciting signal can cause an appreciable shift in resonant frequency peaks. The fluorescent assay method requires fluorescent-labeled antibody/antigen, thereby increasing the chemical cost required for carrying out the test. Requirements of highly skilled personnel and lengthy analysis procedures further limit the viability of most methods.

In order to overcome these drawbacks, we propose a novel method for the detection of *E. coli* bacteria using coplanar waveguide (CPW) as well as distributed MEMS transmission line (DMTL) structures. Previously, MEMS-based CPW sensors have been used for simultaneous detection of concentrations of the organic and inorganic substances in a hybrid fluidic solution [21]. DMTLs for biosensing applications [22, 23] have also been demonstrated. By extending this, we propose a design for pathogenic bacteria detection on the basis of change in wave properties within CPW, in the presence of a bacterium cell on the CPW. We also propose a structure based on DMTL, which allows for more interaction between the electromagnetic waves and measurand. Both methods have a lower response time and allow for very high sensitivity. Selectivity of the sensor can be achieved by immobilizing a functionalization layer of anti-*E. coli* antibody [17]. Since the functionalization layer takes care of the selectivity, labeling agents are not required. With necessary calibration and appropriate functionalization layers, this method can be extended to identify other pathogenic bacteria and biomedical samples, as well as to determine



**Fig. 1** *E. coli* bacteria

their concentration. Using a parallel CPW/DMTL with a pure sample for differential mode analysis, with the sample to be tested can yield accurate results. Such a sensor can be extensively used in hospitals and clinical labs. Incorporating similar sensors in quality control systems of food processing centers and water distribution systems allows for continuous real-time monitoring of product and process quality. Since the sensor can measure the concentration of bacteria, it can also determine the extent of contamination in the sample. Hence, this sensor would be of high industrial value.

In this paper, we first go through the basic theoretical background required to understand the working principle of the sensor. Then, the design of the CPW, DMTL, and *E. coli* bacteria model used for simulation are presented along with different simulation results and their analysis. This is followed by the concluding remarks and the future scope of the study.

## 2 Theoretical Background

### 2.1 Waveguide

A waveguide is a structure which can guide electromagnetic or sound waves. The waveguide confines the wave within the structure by total internal reflection from the waveguide wall and guides the wave in the required direction. In an ideal case, the loss during transmission through a waveguide is zero [24]. Waveguides are used for transmitting signals, for nondestructive evaluation of materials, in microwave oven, and transmitting power between components of a system like radar, radio, or optical devices. Examining chemical/biological samples with the help of waveguides is a recent area of research. Since the properties of the wave through the waveguide also depend upon the properties of the sample placed on the waveguide, the sample can be quantitatively and qualitatively analyzed. The two waveguide structures dealt in this paper are CPW and DMTL.

#### 2.1.1 Coplanar Waveguide

CPW is formed from a conductor separated from a pair of ground planes, atop a dielectric medium [25]. A CPW can be effectively represented as shown in Fig. 2.

$L_t$  and  $C_t$  represent the unloaded inductance and capacitance of the CPW, respectively.

$$C_t = \sqrt{\frac{\varepsilon_{eff}}{c Z_0}} \quad (1)$$

$$L_t = C_t Z_0^2 \quad (2)$$

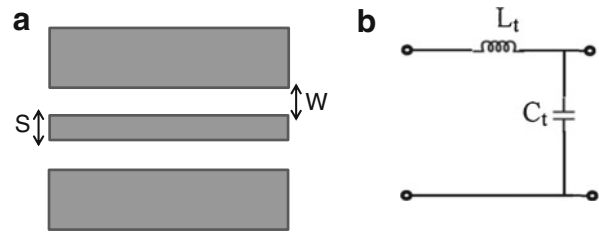


**Fig. 2** Coplanar waveguide: **a** CPW schematic; **b** equivalent circuit of CPW

$c$  is free space electromagnetic wave velocity, and  $\varepsilon_{eff}$  is the effective dielectric constant of the unloaded CPW transmission line.

The characteristic impedance of CPW is given by Eq. (3).

$$Z_0 = \frac{30\pi K(k_0)}{\sqrt{\varepsilon_{eff}} K(k_0)} \quad (3)$$

where

$$\varepsilon_{eff} = 1 + \frac{(\varepsilon_r - 1)}{2} \frac{K(k_1)K(k_0')}{K(k_1')K(k_0)} \quad (4)$$

$$k_0 = \frac{S}{S + 2W} \quad (5)$$

$$k_1 = \frac{\sinh \frac{\pi S}{4h_1}}{\sinh \frac{\pi(S + 2W)}{4h_1}} \quad (6)$$

$$k_0' = \sqrt{1 - k_0^2} \quad (7)$$

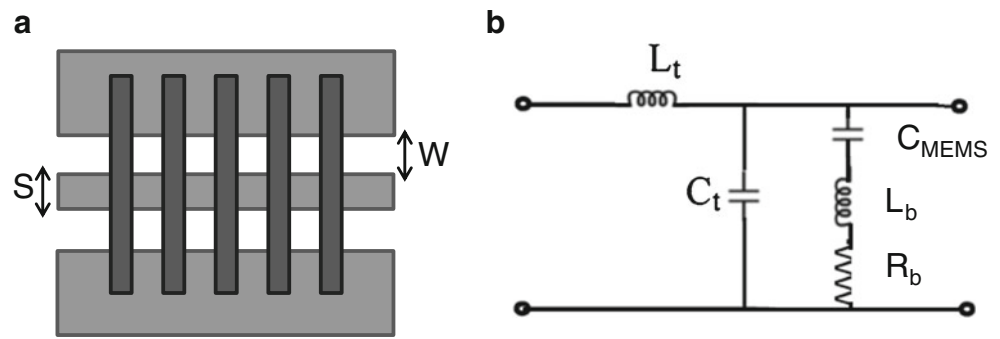
$$k_1' = \sqrt{1 - k_1^2} \quad (8)$$

$\varepsilon_r$	Dielectric constant of the substrate
$K(k)$	Complete elliptical integral of the first kind
$S$	Width of the central conductor
$W$	Width of the gap between central conductor and ground plane
$h_1$	Thickness of the substrate

#### 2.1.2 Distributed MEMS Transmission Line

The DMTL consists of a high impedance line capacitively loaded by the periodic placement of MEMS bridges. The MEMS bridges in a DMTL can be modeled as a lumped-series RLC circuit parallel to CPW as shown in Fig. 3.

**Fig. 3** Distributed MEMS transmission line: **a** DMTL schematic; **b** equivalent circuit of DMTL



$L_t$  and  $C_t$  represent the unloaded inductance and capacitance.  $L_b$ ,  $R_b$ , and  $C_{MEMS}$  refer to the inductance, resistance, and capacitance introduced by the bridges.

## 2.2 VSWR

Voltage standing wave ratio (VSWR) is defined as the maximum value of the RF envelope over the minimum value of the RF envelope. Its relation to  $\rho$  is given in Eq. (9), where  $\rho$  is the real part of the complex reflection coefficient. VSWR ranges from 1 (no reflection) to infinity (full reflection).

$$\text{VSWR} = \frac{1 + \rho}{1 - \rho} \quad (9)$$

## 2.3 S Parameters

Since it is difficult to measure total current or voltage at very high frequencies, scattering parameters (S parameters) are generally measured. These parameters relate to familiar measurements such as gain, loss, and reflection coefficient. They are relatively simple to measure and do not require connection of undesirable loads to the device under test. S parameters are determined by measuring the magnitude and phase of the incident, reflected, and transmitted signals when the output is terminated in a load that is precisely equal to the characteristic impedance of the test system.

The scattering matrix is given by,

$$S = \begin{bmatrix} S_{11} & S_{12} \\ S_{21} & S_{22} \end{bmatrix} \quad (10)$$

where  $S_{11}$  and  $S_{22}$  are reflection parameters and  $S_{21}$  and  $S_{12}$  are transmission parameters.

If  $a_1$  and  $a_2$  are incident waves and  $b_1$  and  $b_2$  are the outgoing waves of a two-port network, then we have the following equations:

$$b_1 = S_{11}a_1 + S_{12}a_2 \quad (11)$$

$$b_2 = S_{21}a_1 + S_{22}a_2 \quad (12)$$

## 3 Design and Modeling

### 3.1 *E. coli* Model

As shown in Fig. 4a, the *E. coli* bacterium was modeled as a three-shell model [26] with an inner protoplasm layer covered by a membrane phase followed by a cell wall. The average dimensions of an *E. coli* bacterium cell are a diameter of 0.68  $\mu\text{m}$  and length of 2.79  $\mu\text{m}$ . The thickness of the membrane is 0.005  $\mu\text{m}$ , and the cell wall is 0.02  $\mu\text{m}$ . The values of relative permittivity, loss tangent, and conductivity were taken from the literature [26]. The values of relative permittivity and bulk conductivity used for each phase are shown in Table 1.

### 3.2 CPW

A coplanar waveguide on a silicon substrate was considered for the study as shown in Fig. 4b. Ground planes and central conductors of the sensor were designed to be made of gold and are 5  $\mu\text{m}$  thick. The width of the ground plane is 262.5  $\mu\text{m}$  and that of the central conductor is 90  $\mu\text{m}$ . The dielectric constant of the silicon substrate is 11.9.

### 3.3 DMTL

Five bridges made of nickel are placed on the CPW, each 220  $\mu\text{m}$  wide and 1.5  $\mu\text{m}$  thick at a height of 5  $\mu\text{m}$  as shown in Fig. 4c. Nickel was chosen for the bridges due to its mechanical strength. The interbridge gap is 320  $\mu\text{m}$ . The dielectric layer on the central conductor was made of silicon nitride due to its good isolation properties [22].

## 4 Simulation

The high-frequency structural simulator, a finite element method solver, was used for simulations. Wave ports were defined on the front and back end of the CPW and DMTL structures. The simulation studies were carried out with and without placing the bacteria on the sensor structure. The



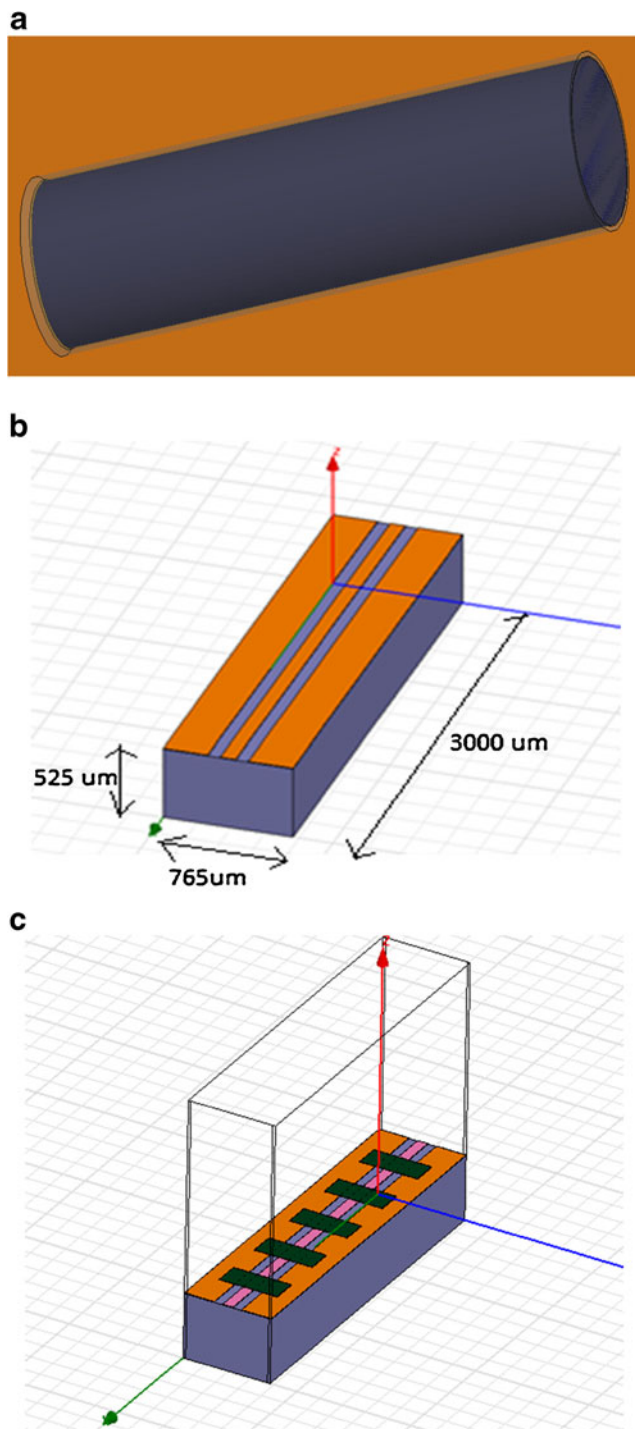


**Fig. 4** Modeling the bacteria and the sensor: **a** *E. coli* bacterium model; **b** coplanar waveguide; **c** distributed MEMS transmission line

bacteria were placed in different numbers and orientation on the sensor structure for further analysis. Simulations were carried out for a wide range of frequencies from 1 to 100 GHz. Table 2 shows the four major situations for which the simulation studies were carried out. Case 2, case 3, and case 4 are shown in Fig. 5a–c, respectively.

**Table 1** Relative permittivity and bulk conductivity of *E. coli* [26]

Sl no.	Phase	Relative permittivity	Bulk conductivity ( $\text{Sm}^{-1}$ )
1	Protoplasm	67	0.17
2	Membrane	9.5	$5\text{e}-8$
3	Cell wall	60	0.73

## 5 Analysis and Discussion

### 5.1 Characteristic Impedance with Bacteria Placed on CPW

Placing a bacterium on the waveguide surface is equivalent to adding a capacitor in parallel with the impedance offered by the CPW. Hence, the effective impedance of the CPW will decrease. This result was verified through simulations as shown in Fig. 6a. The same result can be obtained using Eq. (3). As the number of bacteria on the CPW increases, the effective dielectric constant of the CPW also increases. From Eq. (3), it is clear that this will result in the decrease of characteristic impedance.

### 5.2 S Parameters with Bacteria Placed on CPW

The simulations showed that with increase in number of bacteria on CPW, reflection parameters decreased and transmission parameters increased.  $S_{11}$  and  $S_{22}$  parameters were found to have a larger variation than  $S_{12}$  and  $S_{21}$  parameters. Therefore, it will be easier to monitor reflection parameters for bacteria detection within a range of 1 to 20 GHz while using a CPW. Figure 6b shows the plot of the  $S_{11}$  parameter for different cases under study. The maximum deviation in reflection parameter is found in case 4, at 18 GHz. At 18 GHz,  $S_{11} = -25.92$  dB without the bacterium, whereas for case 4,  $S_{11} = -60.93$  dB.

### 5.3 VSWR with Bacteria Placed on CPW

The VSWR values were found to decrease as the number of bacteria on CPW increased as shown in Fig. 6c. This result

**Table 2** Different cases in simulation

Case no.	Description
Case 1	1 bacteria at the center of central conductor, with axis of the cylinder along the X-axis
Case 2	7 bacteria place along X-axis in the central conductor as shown in Fig. 5a
Case 3	7 bacteria placed along the Y-axis in the central conductor as shown in Fig. 5b
Case 4	Arrangement of $7 \times 7$ bacteria as shown in Fig. 5c

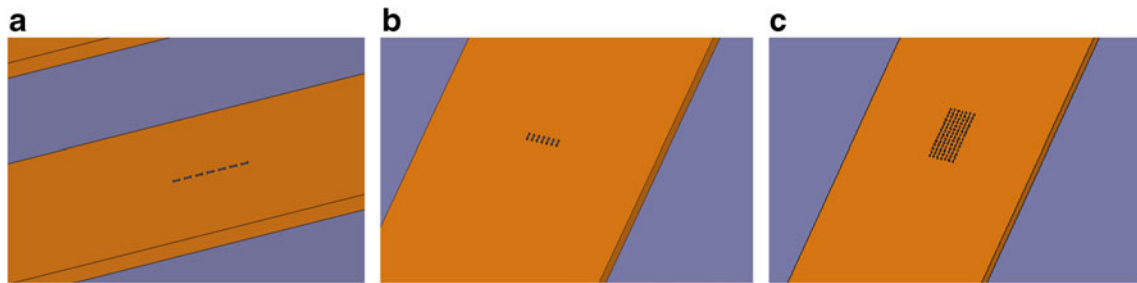


**Fig. 5** Different cases of simulation: **a** case 2, seven bacteria placed along the wave propagation direction; **b** case 3, seven bacteria placed parallel to each other; **c** case 4, seven-by-seven arrangement of bacteria

can be justified by Eq. (9). With increase in number of bacteria, the reflection coefficient decreases as seen from the result of  $S_{11}$  simulations. Hence, VSWR decreases, as

seen from Eq. (9). The maximum deviation was for case 4 at 11 GHz. At 11 GHz, without the bacterium, VSWR=1.2043 whereas for case 4, VSWR=1.0075.

**Fig. 6** RF characteristics with and without the bacteria placed on CPW; **a** characteristic impedance vs. frequency; **b**  $S_{11}$  parameter vs. frequency; **c** VSWR vs. frequency

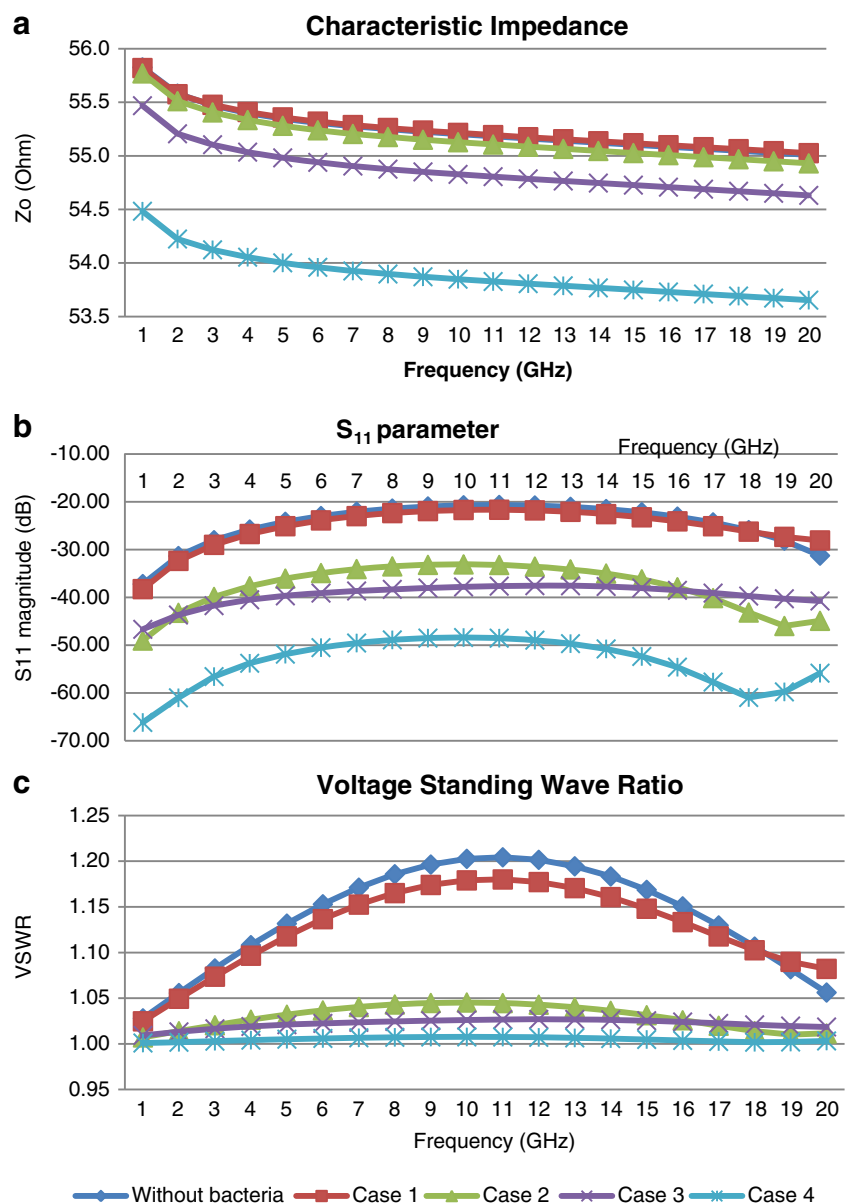
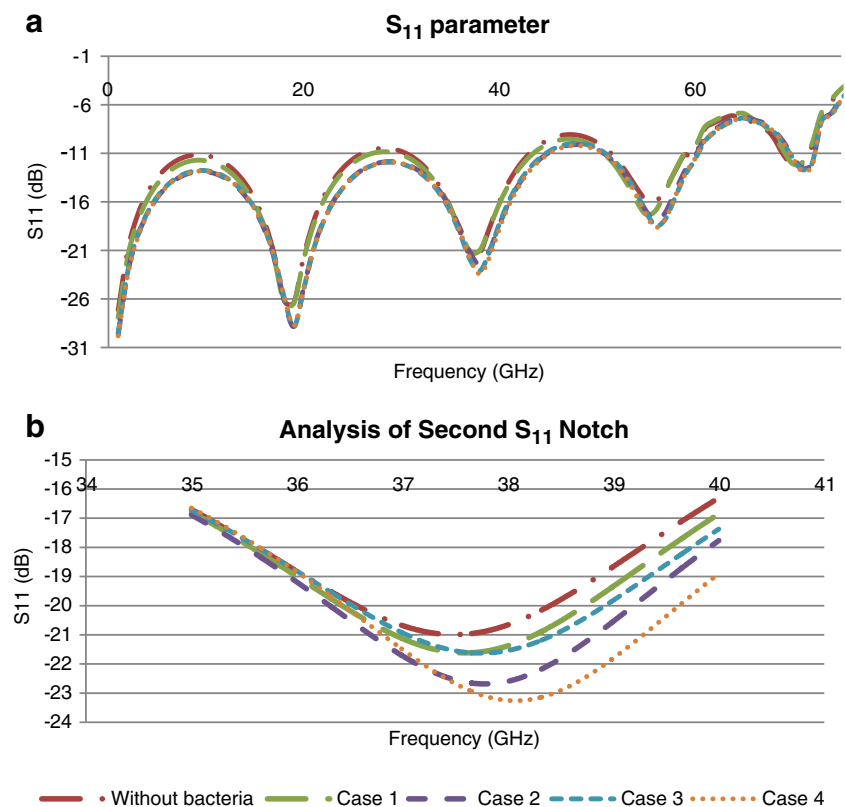


**Fig. 7** Reflection parameter in DMTL with and without bacteria placed on it; **a**  $S_{11}$  parameter vs. frequency; **b** analysis of the second  $S_{11}$  notch



#### 5.4 Shift in Resonance Frequency with Bacteria Placed on DMTL

For the DMTL, the S parameters, VSWR, and  $Z_0$  are in almost close range when the number of bacteria is varied, in comparison to the results that we obtained for CPW. However, the quality factor of the resonant frequency peaks improved in DMTL. From Fig. 7a, it is clear that the first two notches occur at around 18–20 and 35–40 GHz, while using a DMTL.

On close analysis, we find that the frequency shift of the first notch does not yield conclusive results about the presence of bacteria. However, as the number of bacteria increases, the second notch shifts to higher frequency as shown in Fig. 7b. Table 3 gives the resonant frequency of different cases for the second notch.

**Table 3** Resonant frequencies of the notch in the range 35–40 GHz with and without bacteria placed on DMTL

Case	Frequency (GHz)
Without bacteria	37.494
Case 1	37.595
Case 2	37.779
Case 3	37.745
Case 4	38.072

#### 6 Conclusion

A label-free biosensor design for detection of *E. coli* bacteria has been proposed in this paper. We proposed two structures, a CPW and DMTL, upon which the bacteria to be analyzed can be placed. The *E. coli* bacterium cell was modeled as a three-shell structure, where the inner protoplasm is covered by an outer membrane phase and a cell wall. To study the feasibility of the sensor design, CPW as well as DMTL with and without bacteria positioned on it were simulated. The S parameters and VSWR of the CPW were analyzed and were found to vary as the number of bacteria positioned on the CPW increases. With increase in number of bacteria, the VSWR and S parameters decreased. Reflection parameters were found to have more deviation than the transmission parameters. When a DMTL is used, the quality factors of the resonant peaks improved. For the second notch of the resonant frequency of the  $S_{11}$  parameter, the resonant frequency shifts to higher values as the number of bacteria increases. Selectivity towards *E. coli* bacteria can be achieved by immobilizing a layer of anti *E. coli* antibody on the central conductor of CPW/DMTL. Hence, the proposed method can be used for detection of *E. coli* bacteria. With sufficient calibration, this method can be used for measuring the concentration of the bacteria. The proposed method can also be extended for analyzing other bacteria and biomedical samples.

## References

- Ivnitski, D., Hamid, I. A., Atanasov, P., Wilkins, E. (1991). Review—biosensors for detection of pathogenic bacteria. *Biosensors & Bioelectronics*, 14, 599–624. doi:10.1016/S0956-5663(99)00039-1.
- Wang, L., Sipe, D. M., Xu, Y., Lin, Q. (2008). A MEMS thermal biosensor for metabolic monitoring applications. *Journal of Microelectromechanical Systems*, 17, 318–327. doi:10.1109/JMEMS.2008.916357.
- Madou, M., & Florkey, J. (2000). From batch to continuous manufacturing of microbiomedical devices. *Chemical Reviews*, 100, 2679–2692.
- Kima, Y. I., Park, T. S., Kang, J. H., Lee, M. C., Kim, J. T., Park, J. H., et al. (2006). Biosensors for label free detection based on RF and MEMS technology. *Sensors and Actuators B*, 119, 592–599. doi:10.1016/j.snb.2006.01.015.
- Kricka, L. J. (2001). Microchips, microarrays, biochips and nanochips: personal laboratories for the 21st century. *Clinica Chimica Acta*, 307, 219–223. doi:10.1016/S0009-8981(01)00451-X.
- Rangel, J. M., Sparling, P. H., Crowe, C., Griffin, P. M., Swerdlow, D. L. (2005). Epidemiology of *Escherichia coli* O157:H7 outbreaks, United States, 1982–2002. *Emerging Infectious Diseases*, 11, 603–609. doi:10.3201/eid1104.040739.
- Wynter, S. A., & Ivy, J. E. (2009). Simulating public health emergency response: a case study. *Process IEEE Winter Simulation Conference, 2009*, 1957–1986. doi:10.1109/WSC.2009.5429730.
- Nestlé USA (2009). Press release, Nestlé USA's baking division initiates voluntary recall. Nestlé USA, June 19, 2009. <http://www.fda.gov/Safety/Recalls/ucm167954.htm>. Accessed 8 January 2012.
- National Beef Packing Co. LLC (2011). Recall release, National Beef Packing Co. LLC Recall, Indiana State Department of Health. August 15, 2011. [http://www.state.in.us/isdh/files/National\\_Beef\\_Packing\\_Co\\_LLC\\_Recall.pdf](http://www.state.in.us/isdh/files/National_Beef_Packing_Co_LLC_Recall.pdf). Accessed 12 January 2012.
- Gau, J. J., Lan, E. H., Dunn, B., Ho, C. M., Woo, J. C. S. (2001). A MEMS based amperometric detector for *E. coli* bacteria using self-assembled monolayer. *Biosensors & Bioelectronics*, 16, 745–755. doi:10.1016/S0956-5663(01)00216-0.
- Polyzoev, V., Enikov, E., Heinze, B., Yoon, J. Y. (2009). Magnetic particle enhanced microcantilever biosensor for rapid and sensitive *E. coli* detection. *IEEE/ISOT International Symposium on Optomechatronic Technologies* 387–391. doi:10.1109/ISOT.2009.5326138.
- Bakar, M. H. A., Ibrahim, M. H., Kassim, N. M., Mohammad, A. B. (2009) A preliminary investigation on MEMS based immunosensor for *E. coli* O157:H7 detection. *Proc. IEEE 9th Malaysia International Conference on Communications* 51–54. doi:10.1109/MICC.2009.5431414.
- Zhu, P., Shelton, D. R., Karns, J. S., Sundaram, A., Li, S., Amstutz, P., et al. (2005). Detection of water-borne *E. coli* O157 using the integrating waveguide biosensor. *Biosens Bioelectron*, 21, 678–683. doi:10.1016/j.bios.2005.01.005.
- Berkenpas, E., Kenny, T., Millard, P., Cunha, M. P. D. (2005). A langasite SH SAW O157:H7 *E. coli* sensor. *IEEE Ultrasonics Symposium, 1*, 54–57.
- Chaudhuri, C. R., Das, R. D., Dey, S., Das, S. (2011). Functionalised silicon microchannel immunosensor with portable electronic readout for bacteria detection in blood. *IEEE Sensors J.* 323–326. doi:10.1109/ICSENS.2011.6127364.
- Huang, X. J., & Zhang, Y. Y. (2006). Electrical determination of *E. coli* O157:H7 using tin-oxide nanowire coupled with microfluidic chip. *IEEE Sensors J.* 6, 1376–1377. doi:10.1109/JSEN.2006.884433.
- Dastider, S. G., Barizuddin, S., Wu, Y., Dweik, M., Almasri, M. (2013). Impedance biosensor based on interdigitated electrode arrays for detection of low levels of *E. coli* O157:H7. *MEMS 2013*, Taipei, Taiwan. doi:10.1109/MEMSYS.2013.6474404.
- Lee, J. Y., Park, E. J., Min, N. K., Pak, J. J., Lee, C. J., Kim, M. J., et al. (2009). Carbon nanotube based electrochemical immunosensors for high-sensitive detection of *E. coli*. *IEEE Sensors 2009 Conference*, 1176–1179. doi:10.1109/ICSENS.2009.5398352.
- Wu, Y., Hu, F., Gan, N., Li, T., Gao, L. (2010). One novel composite nano-particles membrane modified amperometric immunosensor for *Escherichia coli* in polluted waters. *3rd International Conference on Biomedical Engineering and Informatics*, 2010. doi:10.1109/BMEI.2010.5639388.
- Yang, Y., Kim, S., Chae, J. (2011). Separating and detecting *Escherichia coli* in a microfluidic channel for urinary tract infection applications. *Journal of Microelectromechanical Systems*, 20, 819–827. doi:10.1109/JMEMS.2011.2159095.
- Li, L. J. (2010). Simultaneous detection of organic and in-organic substances in a mixed aqueous solution using a microwave dielectric sensor. *Progress In Electromagnetics Research C*, 14, 163–171. doi:10.2528/PIERC10051308.
- Li, L., & Uttamchandani, D. (2009). A microwave dielectric biosensor based on suspended distributed MEMS transmission lines. *IEEE Sensors Journal*, 9, 1825–1830. doi:10.1109/JSEN.2009.2031388.
- Li, L., & Uttamchandani, D. (2009). Flip-chip distributed MEMS transmission lines (DMTLs) for bio sensing applications, *IEEE Trans. Industrial Electronics*, 56, 986–990. doi:10.1109/TIE.2008.2003204.
- Sadiku, M. N. (2005). *Elements of electromagnetics*. USA: Oxford University Press.
- Simons, R. N. (2001). *Coplanar waveguide circuits, components, and systems*. Cleveland: Wiley.
- Asami, K., Hanai, T., Koizumi, N. (1980). Dielectric analysis of *Escherichia coli* suspensions in the light of the theory of interfacial polarization. *Biophysical Journal*, 31, 215–228. doi:10.1016/S0006-3495(80)85052-1.